Option Pricing for a Stochastic-Volatility Jump-Diffusion Model

Guoqing Yan*

and

Floyd B. Hanson*

Department of Mathematics, Statistics, and Computer Science

University of Illinois at Chicago

Conference on Stochastic Control & Numerics
University of Wisconsin-Milwaukee
15 September 2005

* **This material is based upon work supported by the National Science Foundation under Grant No. 0207081 in Computational Mathematics. Any opinions, findings, and conclusions or recommendations expressed in this material are those of the author(s) and do not necessarily reflect the views of the National Science Foundation.**

Outline

1. Introduction.

2. Stochastic-Volatility Jump-Diffusion Model.

3. European Option Prices.

4. Computing Fourier integrals.

5. Numerical Results.

6. Conclusions.

1. Introduction

- Classical Black-Scholes (1973) model fails to reflect the three empirical phenomena:
  - Asymmetric leptokurtic features: return distribution skewed left, has a higher peak and heavier tails than normal distribution;
  - Volatility smile: implied volatility not constant as in B-S model;
  - Large, sudden movements in prices: crashes and rallies.
- Recently empirical research (Andersen et al.(2002), Bates (1996) and Bakshi et al.(1997)) imply that most reasonable model of stock prices includes both stochastic volatility and jump diffusions. Stochastic volatility is needed to calibrate the longer maturities and jumps are needed to reflect shorter maturity option pricing.
- log-uniform jump amplitude distribution is more realistic and accurate to describe high-frequency data; square-root stochastic volatility process allow for systematic volatility risk and generates an analytically tractable method of pricing options.

2. Stochastic-Volatility Jump-Diffusion Model

- Assume asset price $S(t)$, under a risk-neutral probability measure $\mathcal{M}$, follows a jump-diffusion process and conditional variance $V(t)$ follows a square-root mean-reverting diffusion process:

$$dS(t) = S(t)\left((r - \lambda\bar{J})dt + \sqrt{V(t)}dW_s(t) + J(Q)dN(t)\right), \quad (1)$$

$$dV(t) = k\left(\theta - V(t)\right)dt + \sigma\sqrt{V(t)}dW_v(t). \quad (2)$$

where

  - $r =$ constant risk-free interest rate;
  - $W_s(t)$ and $W_v(t)$ are standard Brownian motions with correlation: $\mathrm{Corr}[dW_s(t), dW_v(t)] = \rho$;
  - $J(Q) =$ Poisson jump-amplitude, $Q =$ underlying Poisson amplitude mark process selected so that $Q = \ln(J(Q) + 1)$;
  - $N(t) =$ compound Poisson jump counting process with jump intensity λ.

- Density of jump-amplitude mark Q is uniformly distributed:

$$\phi_Q(q) = \frac{1}{b-a} \left\{ \begin{array}{ll} 1, & a \le q \le b \\ 0, & \text{else} \end{array} \right\} ,$$

  - Mark Mean: $\mu_j \equiv \mathrm{E}_Q[Q] = 0.5(b+a)$;
  - Mark Variance: $\sigma_j^2 \equiv \mathrm{V}ar_Q[Q] = (b-a)^2/12$;
  - Jump-Amplitude Mean:

$$\bar{J} \equiv \mathrm{E}[J(Q)] \equiv \mathrm{E}[\exp(Q)-1] = (\exp(b)-\exp(a))/(b-a)-1.$$

- By Itô's chain rule, log-return process $\ln(S(t))$ satisfies SDE:

$$d\ln(S(t)) = (r - \lambda\bar{J} - V(t)/2)dt + \sqrt{V(t)}dW_s(t) + QdN(t)\ . \quad (3)$$

3. European Option Prices

3.1 Probability Distribution Function:

- Price of European call option under risk-neutral probability measure:

$$\begin{aligned} C(S(t),V(t),t;K,T) &= e^{-r(T-t)}\mathrm{E}_{\mathcal{M}}[\max[S_T-K,0]|S(t),V(t)] \\ &= S(t)P_1(S(t),V(t),t;K,T) \\ &\quad -Ke^{-r(T-t)}P_2(S(t),V(t),t;K,T); \end{aligned} \tag{4}$$

- $C(S(t),V(t),t;K,T)e^{r(T-t)} = \mathrm{E}_{\mathcal{M}}[\max(S_T-K,0)|S(t),V(t)] =$ conditional expectation of the composite process;
- Change of variables: $L(t)=\ln(S(t))$ and $\kappa=\ln(K)$, so $\widehat{C}(L(t),V(t),t;\kappa,T)\equiv C(S(t),V(t),t;K,T)$ in terms of processes or for PDEs $\widehat{C}(\ell,v,t;\kappa,T)\equiv C(\exp(\ell),v,t;\exp(\kappa),T)$;
- Applying the two-dimensional Dynkin theorem, using $\mathcal{A}$ as

backward operator:

$$
\begin{aligned}
0 \quad = \quad & \frac{\partial \widehat{C}}{\partial t} + \mathcal{A}[\widehat{C}](\ell, v, t; \kappa, T) \equiv \frac{\partial \widehat{C}}{\partial t} + \left(r - \lambda \bar{J} - \frac{1}{2} v \right) \frac{\partial \widehat{C}}{\partial \ell} \\
& + k(\theta - v) \frac{\partial \widehat{C}}{\partial v} + \frac{1}{2} v \frac{\partial^2 \widehat{C}}{\partial \ell^2} + \rho \sigma v \frac{\partial^2 \widehat{C}}{\partial \ell \partial v} + \frac{1}{2} \sigma^2 v \frac{\partial^2 \widehat{C}}{\partial v^2} - r \widehat{C} \\
& + \lambda \int_{-\infty}^{\infty} \left(\widehat{C}(\ell + q, v, t) - \widehat{C}(\ell, v, t) \right) \phi_Q(q) dq, \qquad (5)
\end{aligned}
$$

and by substituting and separating variables, produce:

- PIDE for P_1, with boundary condition $\widehat{P}_1(\ell, v, T; \kappa, T) = 1_{\ell > \kappa}$:

$$
\begin{aligned}
0 = & \frac{\partial \widehat{P}_1}{\partial t} + \mathcal{A}_1[\widehat{P}_1](\ell, v, t; \kappa, T) \equiv \frac{\partial \widehat{P}_1}{\partial t} + \mathcal{A}[\widehat{P}_1](\ell, v, t; \kappa, T) + v \frac{\partial \widehat{P}_1}{\partial \ell} \\
& + \rho \sigma v \frac{\partial \widehat{P}_1}{\partial v} + \left(r - \lambda \bar{J} \right) \widehat{P}_1 + \lambda \int_{-\infty}^{\infty} (e^q - 1) \widehat{P}_1(\ell + q, v, t) \phi_Q(q) dq; \qquad (6)
\end{aligned}
$$

- PIDE for P_2, with boundary condition $\widehat{P}_2(\ell, v, T; \kappa, T) = 1_{\ell > \kappa}$:

$$
0 = \frac{\partial \widehat{P}_2}{\partial t} + \mathcal{A}_2[\widehat{P}_2](\ell, v, t; \kappa, T) \equiv \frac{\partial \widehat{P}_2}{\partial t} + \mathcal{A}[\widehat{P}_2](\ell, v, t; \kappa, T) + r \widehat{P}_2; \qquad (7)
$$

3.2 Characteristic Function:

- Corresponding characteristic functions defined by

$$f_j(\ell, v, t; y, T) \equiv -\int_{-\infty}^{\infty} e^{iy\kappa} d\widehat{P}_j(\ell, v, t; \kappa, T), \tag{8}$$

- Satisfying the same PIDEs as the $\widehat{P}_j(\ell, v, t; \kappa, T)$:

$$\frac{\partial f_j}{\partial t} + \mathcal{A}_j[f_j](\ell, v, t; \kappa, T) = 0, \tag{9}$$

where $\mathcal{A}_j$ represents the corresponding full backward operators in (6) and (7) with boundary conditions, $f_j(\ell, v, T; y, T) = +e^{iy\ell}$, respectively for $j = 1:2$.

- Solution conjecture:

$$f_j(\ell, v, t; y, t+\tau) = \exp\left(g_j(\tau) + h_j(\tau)v + iy\ell + \beta_j(\tau)\right), \tag{10}$$

with $\beta_j(\tau) = r\tau\delta_{j,2}$ and boundary conditions $g_j(0) = 0 = h_j(0)$ for $j = 1:2$.

3.3 Solution:

- For the Fourier transforms f_j for $j = 1 : 2$,

$$h_j(\tau) = \frac{(\eta_j^2 - \Delta_j^2)(e^{\Delta_j \tau} - 1)}{\sigma^2(\eta_j + \Delta_j - (\eta_j - \Delta_j)e^{\Delta_j \tau})}; \tag{11}$$

$$\begin{aligned} g_j(\tau) \quad &= \quad ((r - \lambda \bar{J})iy - \lambda \bar{J}\delta_{j,1} - r\delta_{j,2})\tau \\ &\quad + \lambda\tau \int_{-\infty}^{\infty} (e^{(iy+\delta_{j,1})q} - 1)\phi_Q(q)dq \\ &\quad - \frac{k\theta}{\sigma^2}\left(2\ln\left(1 - \frac{(\Delta_j + \eta_j)(1 - e^{-\Delta_j \tau})}{2\Delta_j}\right) + (\Delta_j + \eta_j)\tau\right), \end{aligned} \tag{12}$$

where

$$\eta_j = \rho\sigma(iy + \delta_{j,1}) - k \;\; \& \;\; \Delta_j = \sqrt{\eta_j^2 - \sigma^2 iy(iy \pm 1)};$$

$$\int_{-\infty}^{\infty} (e^{(iy+1)q} - 1)\phi_Q(q)dq \;\; = \;\; \frac{e^{(iy+1)b} - e^{(iy+1)a}}{(b-a)(iy+1)} - 1.$$

- The tail probabilities P_j for $j = 1 : 2$ are

$$P_j(S(t), V(t), t; K, T) = \frac{1}{2} \tag{13}$$

$$+\frac{1}{\pi}\int_{0+}^{+\infty} \mathrm{Re}\left[\frac{e^{-iy\ln(K)} f_j(\ln(S(t)), V(t), t; y, T)}{iy}\right] dy,$$

by complex integration on equivalent contours yielding a residue of $1/2$ and a principal value integral in the limit to the left of the apparent singularity at $y = 0^+$, since the integrand is bounded in the singular limit.

4. Computing Fourier Integrals

4.1 Using 10-point Gauss-Legendre formula for DFTs:

Re-write the Fourier integral as

$$I(x) = \int_0^\infty F(x)dx = \lim_{N->\infty} \sum_{j=1}^{N} \int_{(j-1)h}^{jh} F(x)dx. \tag{14}$$

- Because of singularity at $y = 0$ and oscillatory behavior, discrete Fourier tranform (DFT) sub-integrals in (14) are computed by means of a highly accurate, ten-point Gauss-Legendre formula, which is also an open formula, not evaluating the function at the endpoints.
- N is not fixed but determined by a local stopping criterion: the integration loop is stopped if the ratio of the contribution of the last strip to the total integration becomes smaller than 0.5e-7.
- Step size $h = 5$: Good choice for fast convergence and good precision.

4.2 Using Fast Fourier Transform (FFT):

(After Carr and Madan (1999))

- Initial call option price:

$$C(S(t),V(t),t;K,T) = -\int_K^\infty e^{-r(T-t)}(S(t)-K)dP_2(S(t),V(t),t;K,T); \quad (15)$$

- Modified call option price to remove the singularity:

$$C^{(\mathrm{mod})}(S(t),V(t),t;\kappa,T) = e^{\alpha\kappa}C(S(t),V(t),t;K,T); \quad (16)$$

- Corresponding Fourier transform of $C^{(\mathrm{mod})}(S(t),V(t),t;\kappa,T)$:

$$\Psi(S(t),V(t),t;y,T) = \int_{-\infty}^{\infty} e^{iy\kappa}C^{(\mathrm{mod})}(S(t),V(t),t;\kappa,T)d\kappa; \quad (17)$$

- Thus,

$$C(S(t),V(t),t;K,T) = \frac{e^{-\alpha\kappa}}{\pi}\int_0^\infty e^{-iy\kappa}\Psi(S(t),V(t),t;y,T)dy; \quad (18)$$

$$
\begin{aligned}
\Psi(S(t),V(t),t;y,T) &= -\int_{-\infty}^{\infty} e^{iy\kappa} \int_{\kappa}^{\infty} e^{\alpha\kappa} e^{-r(T-t)} (S(t)-K) \\
&\quad \cdot dP_2(S(t),V(t),t;\kappa,T)d\kappa \\
&= \frac{e^{-r(T-t)} f_2(y-(\alpha+1)i)}{\alpha^2+\alpha-y^2+i(2\alpha+1)y}; \qquad (19)
\end{aligned}
$$

- Transfer the Fourier integral into discrete Fourier transform (DFT) and incorporate Simpson's rule (Carr and Madan (1999)) to increase accuracy of the FFT application:

$$
\begin{aligned}
C(S(t),V(t),t;\kappa,T) = \frac{e^{-\alpha\kappa}}{\pi} \sum_{j=1}^{N} e^{-i\frac{2\pi}{N}jk} e^{iy_j(L-\ln(S))} \Psi(y_j) \\
\cdot \frac{dy}{3}[3+(-1)^{(j+1)}-\delta_j], \qquad (20)
\end{aligned}
$$

where $\alpha = 2.0$ and $dy = 0.25$ are used.

5. Numerical Results

- Two numerical algorithms give the same results within accuracy standard. The FFT method can compute different levels strike price near at-the-money (ATM) in 5 seconds. The standard integration method can give out the results for one specific strike price in about 0.5 seconds. The implementations are using MATLAB 6.5 and on the PC with 2.4GHz CPU.
- The option prices from the stochastic volatility jump diffusion model are compared with those of Black-Scholes model:
  Parameters: $r = 3\%$, $S_0 = \$100$; $\sigma = 7\%$, $V = 0.012$, $\rho = -0.622$, $\theta = 0.53$, $k = 0.012$; $a = -0.028$, $b = 0.026$, $\lambda = 64$.

5.1 Call Prices:

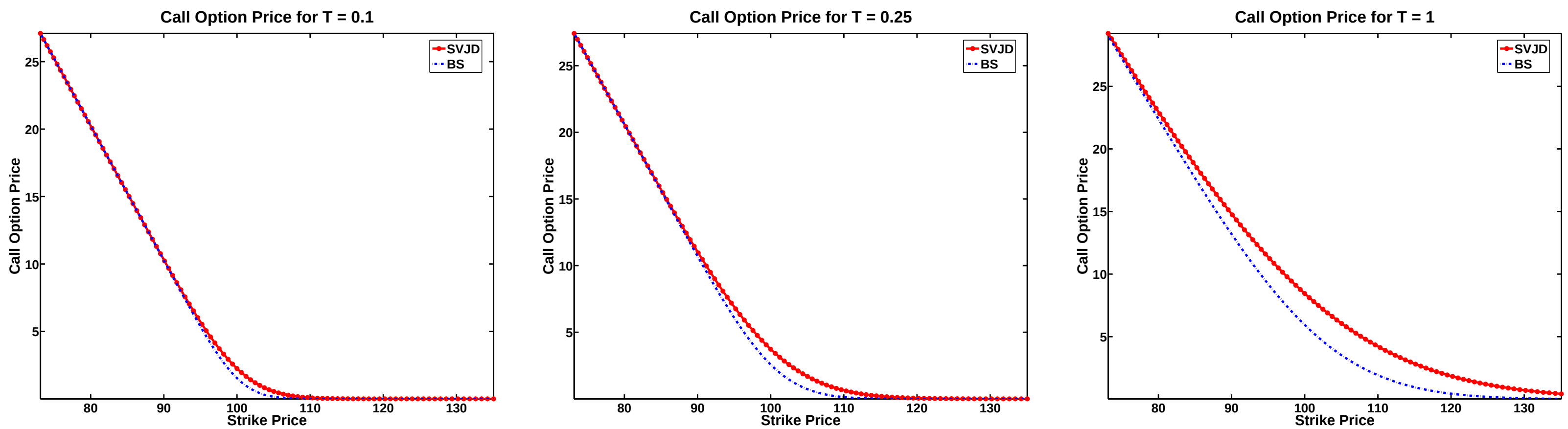

(a) Call option prices for $T = 0.1$.

(b) Call option prices for $T = 0.25$.

(c) Call option prices for $T = 1.0$.

Figure 1: Call option prices for the SVJD model compared to the corresponding pure diffusion Black-Scholes values for $T = 0.1, 0.25, 1.0$.

5.2 Put Prices:

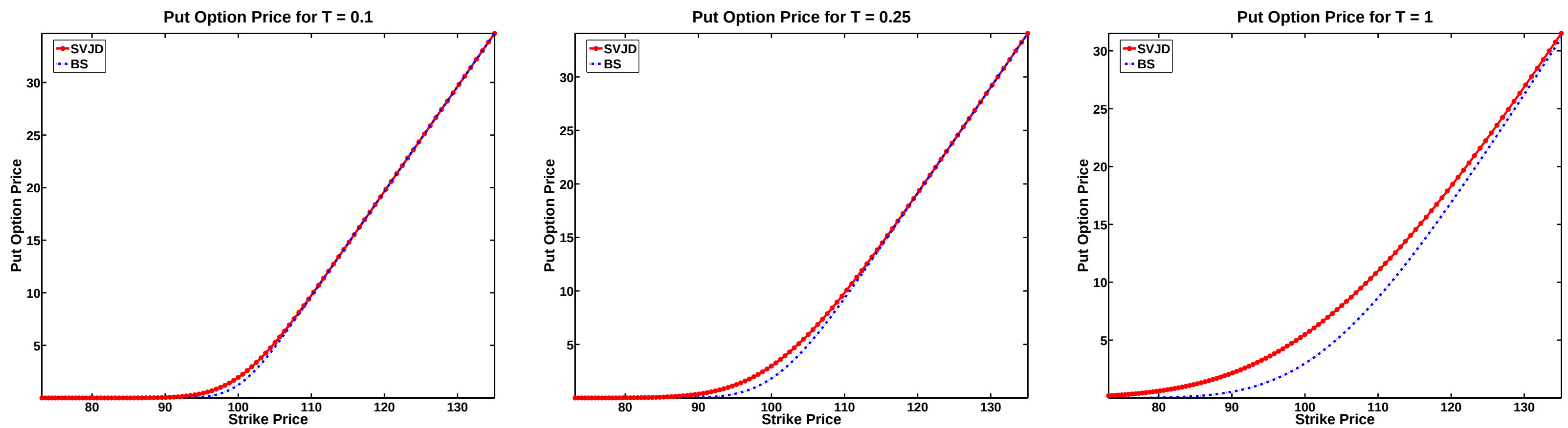

(a) Put option prices for $T = 0.1$.

(b) Put option prices for $T = 0.25$.

(c) Put option prices for $T = 1.0$.

Figure 2: Put option prices for the SVJD model compared to the corresponding pure diffusion Black-Scholes values for $T = 0.1, 0.25, 1.0$.

6. Conclusions

- Proposed an alternative stochastic-volatility, jump-diffusion (SVJD) model, stochastic volatility follows a square-root mean-reverting stochastic process and jump-amplitude has log-uniform distribution.
- Characteristic functions of the log-terminal stock price and the conditional risk neutral probability are analytically derived. The option prices are expressed in terms of characteristic functions in closed form.
- Two numerical computing algorithms using an accurate 10-point Gauss-Legendre Fourier integral (DFT) formula and a fast FFT are implemented. Same option prices are given by two methods for the SVJD model. Compared with those from Black-Scholes model, the SVJD model have higher option prices, especially for longer maturity and near at-the-money (ATM) strike price.